Nanochem. Res., 9(1): 68-76, Winter 2024

RESEARCH PAPER

Three-dimensional ZnS/MoS_2 on cellulose paper for determination of Digoxin in urine and plasma

Marzieh Piryaei*, Mir Mahdi Abolghasemi, Sodabeh Memari

Department of Chemistry, Faculty of Science, University of Maragheh, Maragheh, Iran

ARTICLE INFO

Article History:
Received 25 Sep 2023
Accepted 05 Dec 2023
Published 01 Jan 2024

Keywords:
Thin film microextraction,
Cellulose paper,
ZnS,
MoS2,
HPLC.

ABSTRACT

The current study describes the in-situ growth of ZnS/MoS_2 on cellulose paper using the thin-film microextraction (TFME) method. On cellulose paper, ZnS/MoS_2 was grown using a simple, easy, and inexpensive hydrothermal method. The digoxin was quantified after TFME using high-performance liquid chromatography-UV detection (HPLC-UV). The effect of effective parameters such as extraction time, extraction temperature, agitation speed, and sample ionic strength was investigated, and the best conditions were selected. Under ideal conditions, a calibration curve with good linearity (R^2=0.987) and a low limit of detection (LOD) in the range of 0.01–100 ng mL^{-1} was obtained. The detection limits were 0.03 ng mL^{-1}. For the digoxin, the relative standard deviations (RSDs) were 5.3%. The method was successfully applied to the study of urine and plasma. Relative recoveries were found to range between 96% and102 %. The proposed method provided a straightforward, efficient, and environmentally friendly way for determining digoxin in real-world samples.

How to cite this article
Piryaei M., Abolghasemi M. M., Memari S., Three-dimensional ZnS/MoS2 on cellulose paper for determination of Digoxin in urine and plasma. Nanochem. Res., 2024; 9(1): 68-76. DOI: 10.22036/NCR.2024.01.08

INTRODUCTION

Cardiotonic glycosides have been employed in the treatment of cardiac diseases and failure, particularly atrial arrhythmias. There is an extensive usage of digoxin as a prescribed cardiac glycoside (Fig. 1), for treating congestive heart failure. Owing to the narrow margin between toxic and therapeutic doses, digoxin normally creates side effects. Generally, the adverse digoxin reactions are dose-based occurring at doses greater than those required to obtain the therapeutic effects. Due to the lower therapeutic digoxin index (0.5-2.0 $ngm1^{-1}$), the precise measurement of digoxin concentrations is imperative [1-3].

Several approaches have been reported for digoxin quantitation such as high-performance liquid chromatography (HPLC), radioimmunoassay, fluorescence detection, optical sensor, and LC-MS assay. Several reports have described HPLC techniques to identify and quantify digoxin-like, digoxin metabolites, digoxin substances within biological matrices; however, they are normally not sensitive enough to quantitate lower levels of digoxin (in ng/mL level). Thus, extraction and preconcentration of digoxin in real samples is critical for the determination of digoxin. Recently, developing accurate, sensitive, and fast approaches for quantitative and qualitative analysis of complex specimens has become a key issue. Regardless of the progress in developing highly sensitive analytical tools for analyzing environmental, biological, pharmaceutical, and food products, analytes were unsuccessfully determined in the complicated media. Thus, pretreatment is required for the concentration and extraction of analytes from complex matrices [4-10].

* Corresponding Author Email: *m.piriyaei@gmail.com*

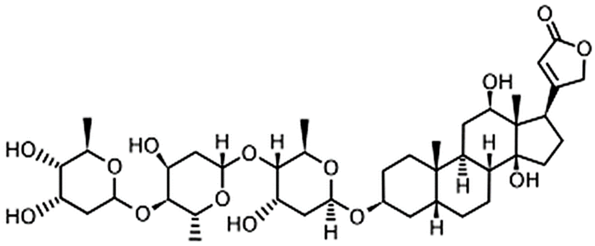

Fig. 1. Molecular structure of digoxin.

Generally, enrichment and separation operations occur through adsorption on liquid-liquid extraction processes and a solid phase. Classic sample preparation techniques have disadvantages such as difficulty in the automation of traditionally liquid or solid-phase extraction methods with great use of the sample amounts and organic liquids as well as being complicated and time-consuming. Utilizing considerable quantities of organic solvents and harmful chemicals contributes to environmental pollution, additional operating costs, health risks on laboratory staff, and waste treatment. Perfect sample separation methods should be cost-effective, applicable and rapid, and easily integrated with most analytical tools. Reducing organic solvent volume as an extraction medium to a less quantity and simplifying sample preparing phases are novel trends in this regard. Therefore, there has been a significant increase in attention to these microextraction methods. These methods, offering some advantages, are recently going to replace classic extraction methods. Some benefits have declined using expensive and toxic extracting liquids to microliter levels, not requiring for procedures such as purification and evaporation, high enrichment factor, enrichment and extraction operations, and separation process. Hence, it is allowed to direct injection of extracted specimens to the HPLC and GC and making automation [11-17].

Solid-phase microextraction approaches are quick, sensitive, and simple solventless approaches for preparing samples using an extracting sorbent. The SPME's principle is oriented by the analytes' interactions with the extraction phase (coating) and the sample matrix through desorption and adsorption (based on the coating nature) [17-21]. Mainly, the SPME's extraction efficiency and selectivity depend on the coating's properties, size, and its interactions with the analytes. Moreover, recently, it was highlighted that the SPME extraction initial rate is proportional to the extraction phase's surface area. By increasing the quantity of coating, the extraction efficiency is incremented. Pawliszyn's research group represented this film microextraction (TFME) as an SPME mode to overcome this limitation in 2003 [22, 23]. A wide and thin membrane is used in TFME, as a sorbent for the microextraction process. The higher ratio of surface area/volume along with increasing the extraction phase volume can improve the technique's sensitivity without scarification of the sampling time in comparison to other SPME methods.

Molybdenum disulfide (MoS_2) is a layered transition metal dichalcogenide formed by stacking weakly interacting two-dimensional (2D) MoS_2 layers, similar to graphite. It has the potential to be used in lubricants, supercapacitors, storage batteries, hydrogen production, storage, adsorbents, and as a photocatalytic agent for pollutant degradation or hydrogen production [24, 25].

In this paper, a flower-like MoS_2 ultrathin nanosheet array was grown on a cellulose paper using a straightforward, low-cost hydrothermal method. After that, on the already-prepared MoS2 nanosheets, 3D hierarchically porous ZnS structures grew.

The potential application of the modified cellulose articles as an extraction stage for TFME was evaluated. Digoxin, a cardiac glycoside that is prescribed, was used as a model compound for TFME. Liquid chromatography with fluorescence detection was used to define the compounds under investigation. The extraction capacity of the modified cellulose papers was examined, and comparisons were made. Concerning the method's extraction effectiveness, the effects of various experimental parameters, including sample ionic strength, agitation, extraction time, and desorption condition, were examined. Finally, the SPME technique was successfully applied to the analysis of the urine and plasma samples.

EXPERIMENTAL SECTION

Chemicals, reagents and real samples

From Merck and Sigma-Aldrich, sodium molybdate, zinc chloride, and thiourea were purchased. From the Zahravi Pharmaceutical Company, digoxin was obtained. Digoxin was prepared as a standard stock solution in methanol, and working solutions were prepared by thinning the stock solutions with water. Urine samples were obtained from the neighborhood pathobiology laboratory, while plasma samples were obtained from the blood transfusion center in East Azerbaijan. Whatman supplied cellulose-ashless filter paper.

Apparatus

The morphologies and compositions of the synthesized materials were investigated by scanning electron microscopy (FE-SEM, TESCAN MIRA3-XMU, Brno (Czech Republic)) equipped with an energy-dispersive X-ray spectroscope (EDS). The Knauer HPLC system (Berlin, Germany) was utilized, armed with a model 3950 auto sampler, model 2600 photo diode-array (PDA) detector, model 1000 LC pump, and a vacuum degasser. Using Knauer Clarity Chrom Workstation data achievement software, the data were obtained. A combination of methanol-water (70:30, vv^{-1}) was included in the mobile phase. The injection volume of 20 μL was used while running the pump at a flow rate of 1 $mLmin^{-1}$ at room temperature and a PDA detector (at 220 nm) was employed to monitor the active values. RP-HPLC analysis was performed isocratically at room temperature using a Spherisorb C18 (250×4.6 mm, 5 mm) column (Waters, Elstree, UK). The homemade DC motor agitator with a speed controller was utilized for rotating the TFME holder.

Synthesis of ZnS–MoS_2 on copy cellulose paper

The MoS_2 hydrothermal growth was considered using cellulose paper as the substrates. To prepare the seed solution, 20×10^{-3} M of thiourea and 10 $\times10^{-3}$ M of sodium molybdate were mixed in deionized water. Dipping the paper substrates was performed after drying at 80 °C, in an as-prepared seed solution for 1 hour. A nutrient solution containing 100 $\times10^{-3}$ M thiourea and 50 $\times10^{-3}$ M sodium molybdate was agitated in DI water for 30 minutes. Then, the nutrient solution and the seed-covered cellulose paper were transported to the hydrothermal reactor and it was maintained at 200 °C for 20 hours. The reactor was allowed to cool down naturally, and the resulting black-colored paper was dried at 80 °C. The hydrothermal synthesis was conducted for the ZnS growth on MoS_2 paper. CH_4N_2S and zinc chloride ($ZnCl_2$) were utilized respectively as the S and Zn sources. The MoS_2 paper was submerged in a seed solution containing equimolar concentrations of CH_4N_2S and $ZnCl_2$ in DI water for 60 minutes. Within a hot air oven, the seed-covered MoS_2 paper was dried at 80 °C. Then, the nutrient solution containing the precursors and the MoS_2 paper was transported to a Teflon-lined autoclave and was kept for 60 min at 200 °C. The resulting ZnS–MoS_2 was rinsed with DI water for removing the excess ZnS and drying was performed at 80 °C [26].

TFME procedure

In order to perform TFME, the papers obtained from section 2.3 were cut into the same 1cm×1cm films. The prepared film was connected to the homemade overhead rotating holder and immersed into the extraction vessel occupied with a sample solution of 10.0 mL at pH = 7. Stirring the holder at 60 rpm, the extracting device was detached from the holder after 30.0 min and placed into a homemade glass vial containing 200μL of desorption solvent (methanol). Sonication of the vial was performed for 2.0 min. Ultimately, 20 μL of analyte-enriched eluent was inserted into HPLC-UV. Fig. 2 represents the schema of the microextraction process.

RESULTS AND DISCUSSION

Characterization of the ZnS/MoS_2 /cellulose paper

Interaction of nanomaterials with target compounds depend on their composition, morphology, shape, structure, size, distribution, and spatial arrangement. In this study, ZnS/MoS_2 structures directly grew over the cellulose paper.

FESEM images represented in Fig. 3 denote ZnS–MoS_2 structures on the cellulose paper, illustrating the ZnS nanospheres growth with an average diameter of 150 to 250 nm on the flower like MoS_2 microspheres surfaces within a sporadic mode. Based on the FESEM images (Fig. 3 c), it was found that ZnS nanospheres possess a high surface roughness which seems as a decent interfacial contact between MoS_2 and ZnS. It is obvious that the further growing of MoS_2 and ZnS does not affect the microfibers of the cellulose paper (Fig. 3b). Flower-like structures were created,

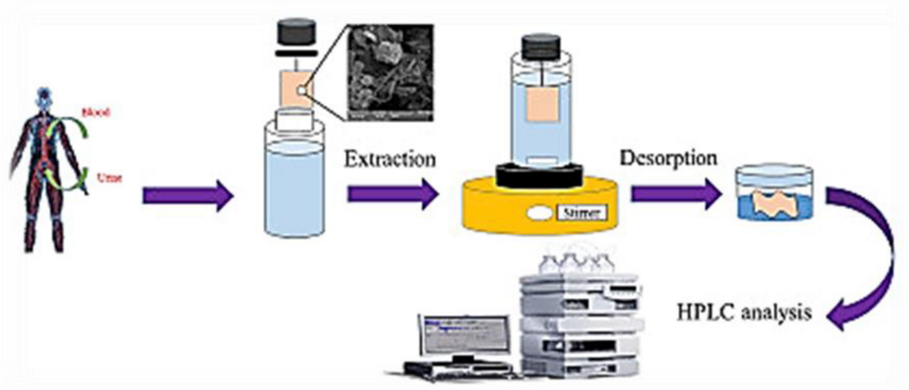

Fig. 2. Thin film extraction of digoxin

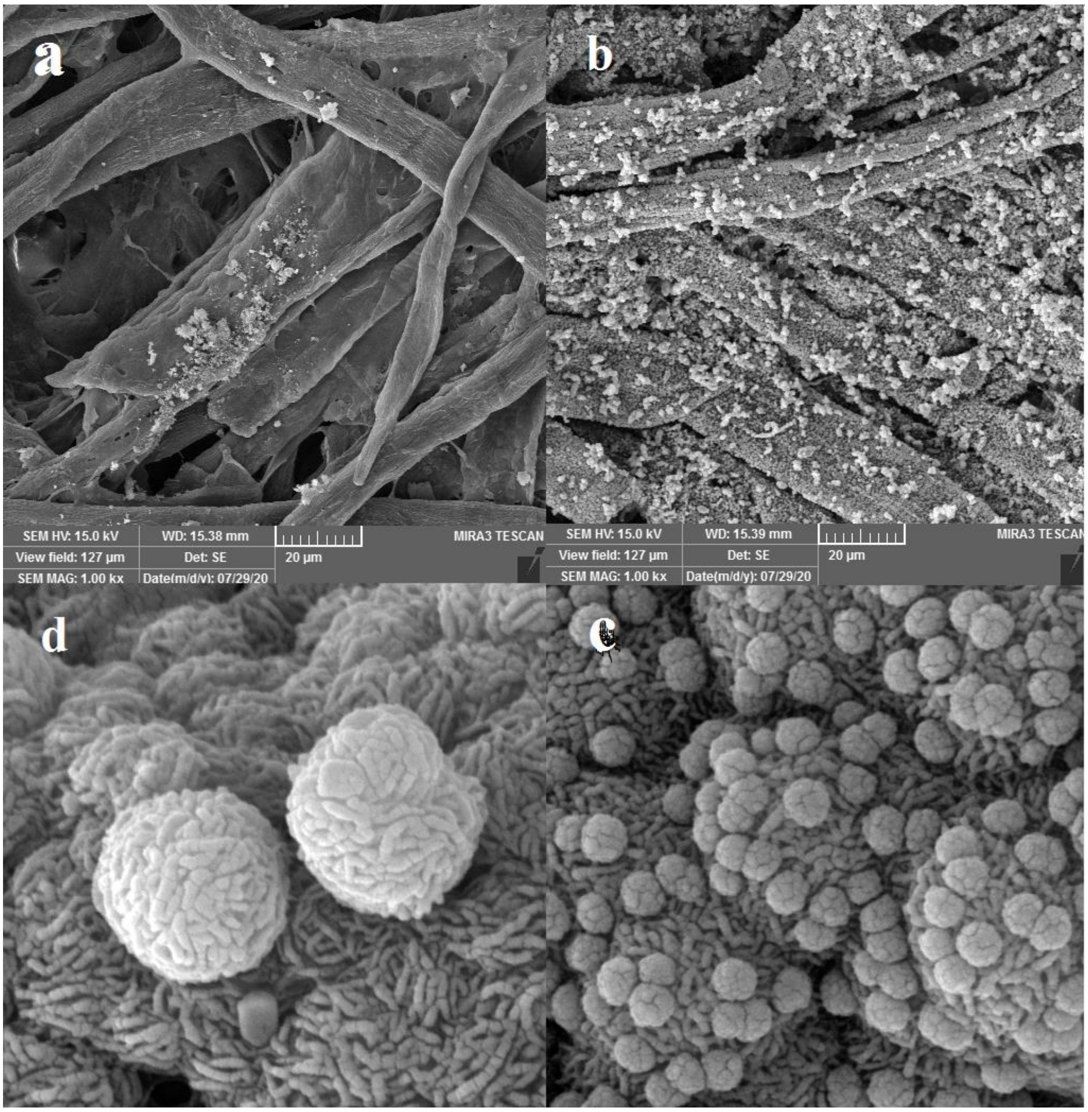

Fig. 3. FESEM images of a) cellulose paper, b) MoS_2 grown on cellulose paper exhibiting micro flower-like structure, c) higher magnification MoS_2 on cellulose paper, d) ZnS on MoS_2-cellulose paper) higher magnification ZnS on MoS_2 cellulose paper.

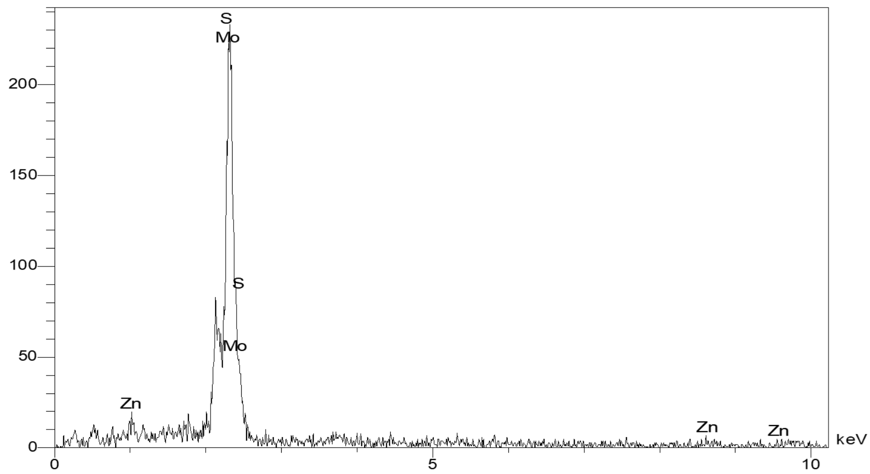

Fig. 4. EDX pattern of the obtained ZnS on MoS2-cellulose paper

Table 1. Quantitative results of EDS analysis for of molybdenum (Mo), zinc (Zn), Sulfur (S) elements across the ZnS on MoS_2-cellulose paper

Element	Atomic % [a]	Weight % [b]
Mo	47.42	70.14
Zn	7.53	7.59
S	45.05	22.27
Totals	100.00	100.00

[a] Atomic Percentage
[b] Weight Percentage

characterized by relatively deep porous and highly open nanostructures. These structures increase the surface area of the grains surface, optimizing the adsorption presses.

To further confirm the formation of the hybrid, elemental composition analysis was performed. The elemental composition analysis was also investigated via energy-dispersive X-ray spectroscopy (Fig. 4). According to Table 1, the only elements observed at the ZnS/MoS_2/cellulose paper were Mo (70.14%) Zn (7.59%) and S (22.27%).

X-ray diffraction (XRD) was applied to study the crystal structure of the as-grown MoS_2 and ZnS/MoS_2 (image not shown). The MoS_2's diffraction peaks are well-consistent with the JCPDS card no. 37-1492, indicating the MoS_2 hexagonal phase. Two extensive peaks equivalent to (100) and (110) planes were found for pristine MoS_2. The peak enlargement might be caused by the synthesis temperature (200 °C). At 2θ ≈14°, the (002) plane reflection is not considered, attributed to the existence of a few-layer (equal or less than 5) MoS_2 or graphene-like MoS_2. The prominent peaks of MoS2 for ZnS–MoS_2 hybrids are reserved and further ZnS diffraction peaks were identified. The ZnS diffraction pattern is matched with the wurtzite (hexagonal) ZnS (JCPDS No. 36-1450). Moreover, the prominent peaks at 2θ ≈22° and 16° were found in both the pristine MoS2 and ZnS–MoS2 hybrids allocated to cellulose paper. The existence of cellulose diffraction peaks indicates the immunity of the substrate paper for degradation within the hydrothermal procedure [25-27].

The wettability of ZnS–MoS_2 on the cellulose paper was investigated. In general, the solid surface is regarded as hydrophilic by the water contact angle (θc) of < 90°, and it is hydrophobic when the water contact angle is >90°. According to Fig. 5, modified ZnS/MoS_2/cellulose paper's hydrophobicity (θc= 48.7°) is higher compared to the bare cellulose paper (θc~0°). Preliminary experiments indicated that the digoxin possessed no affinity for adsorbing over the bare cellulose paper surface. The results demonstrated that the hydrophobicity of the ZnS/MoS_2/cellulose paper increased. Digoxin structure is fraught with polar

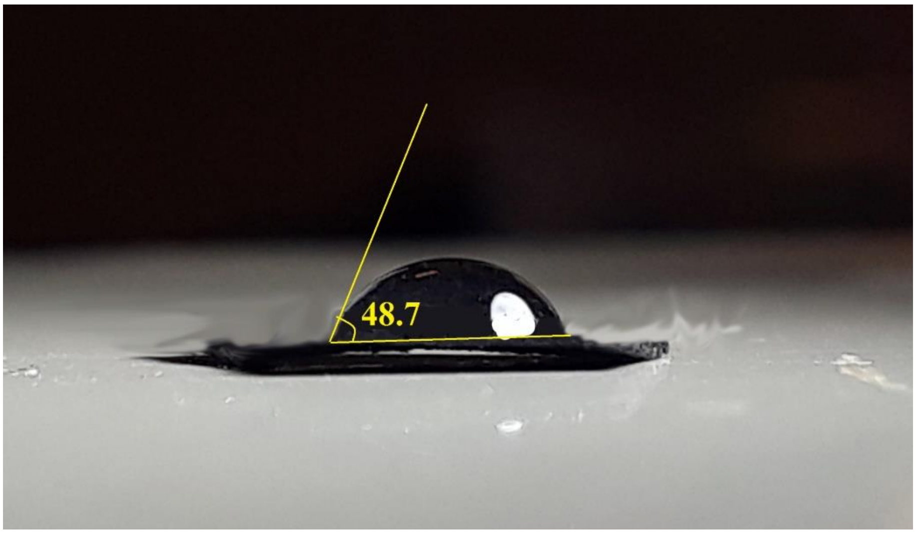

Fig. 5. Photographs of cross sectional view of water drop profile on the surface of ZnS on MoS_2 cellulose paper.

functional groups (OH groups) and its log Kow is 1.26. Therefore, the synergistic effect resulting from the development of hydrophobicity and increase of surface area on ZnS/MoS2 modified cellulose paper enhanced the interaction for adsorption of digoxin in nano-composite structures.

Optimization of TFME conditions

pH effect

Digoxin has acid-base properties, and pH has a significant impact on how easily it can be extracted. For this reason, the impact of pH was examined. The extraction process is significantly influenced by the pH of the solution. Additionally, the pH of the sample solution acts as the primary factor in accelerating the transfer of digoxin from the sample solution to the thin film. As a result, the effects of pH values ranging from 4 to 9 were examined by adding the appropriate amount of sodium hydroxide solution or hydrochloric acid to the aqueous phase. At pH 7, the maximum effectiveness was attained. Digoxin's acid-base equilibrium significantly shifts at low and high pH levels toward neutral types with elevated affinities for the sorbent, increasing the extraction efficiency.

The extraction time effects

TFME is a non-exhaustive extraction method, where the analytes are divided between the extracting phase and sample solution until reaching equilibrium. Thus, extraction time is a key factor that should be assessed. It is worth noting that the TFME method is faster compared to the other SPME processes. In the current work, various extraction times from 1 to 12 minutes were examined. The analytes quantity extracted by the technique was incremented by the sampling time of more than 5 minutes, over which it was almost unaltered (Fig. 6). Thus, a time of 10 minutes was selected as the equilibrium time for analytes extraction.

Effects of agitator's speed

Simplicity is one of the benefits of the TFME method. It has been indicated that this method is performed with no further tool such as syringe (microextraction techniques in some liquid phase) or holder (in traditional SPME). Therefore, several specimens can be prepared instantaneously by the technique. A homemade DC controller agitator armed with a holder was applied for agitating the thin films over extracting. The effects of the agitator's stirring rate for extraction stages were investigated. For microextraction of the digoxin, the agitator's speed of 50 rpm were chosen.

Effects of ionic strength

Within the solid phase microextraction methods, the addition of salt revealed a positive impact and promoted extraction efficiency of several analytes, chiefly polar compounds. Nevertheless, reducing the extraction of the analytes is occasionally found by improving the sample's ionic strength. According to the experimental findings, adding salt into the sample solution reduced the method's extraction efficiency. Adsorption of salt over the modified cellulose paper's surface probably decreases the

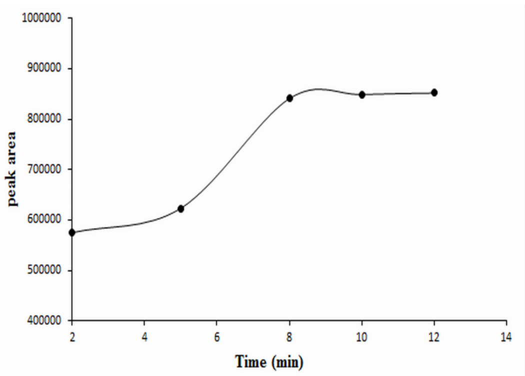

Fig. 6. The effects of the extraction time on the digoxin peak area.

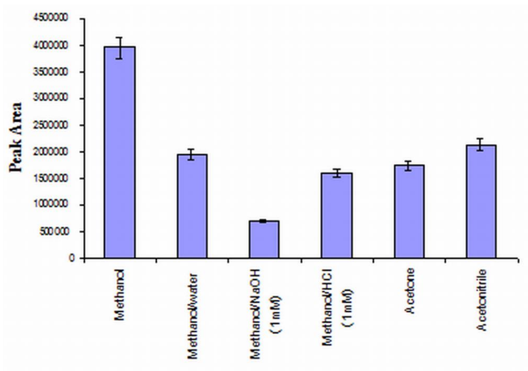

Fig. 7. Effect of type of desorption solvents on the extraction of the digoxin in optimum conditions.

Table 2. Some analytical data obtained for thin film microextraction of Digoxin.

Compound	DLR [a] ($ng\ mL^{-1}$)	Regression coefficient	LOD [b] ($ng\ mL^{-1}$)	Repeatability R.S.D. [c] %, ($1ng\ mL^{-1}$)	Reproducibility R.S.D. %, ($1ng\ mL^{-1}$)
Digoxin	0.01-100	0.987	0.003	5.3	8.7

[a] Dynamic Linear Rang.
[b] Limit of detection calculated as three times the baseline noise.
[c] Relative Standard Deviation

extraction efficiency. Thus, further tests were conducted without adding salt to the specimens.

Optimization of the eluent type, volume and elution time

In order to back-extract the adsorbed analytes, liquid desorption strategy was utilized. In this strategy, the type of desorption solvent plays a major role in improving the efficiency of the method. To increase the extraction efficiency of the method, the type of eluent was optimized. The effect of desorption solvent type on the desorption of digoxin on the sorbent was examined using different solvent including methanol, methanol containing NaOH and HCl (1.0 mM), acetone, and acetonitrile. Experiments were repeated three times under the same condition, and based on the results shown in Fig. 7, methanol gave the best efficiency. To find out the minimum volume of the solvent needed for desorbing efficient analytes, various solvent volumes were assessed within 50 to 400 μL. According to the results, a volume of 200 μL was used for future experiments.

Quantitative evaluation and real sample analysis

The analytical performances of the method were studied (Table 2). A linear function of concentration between 0.01–100 ng mL^{-1} and a correlation coefficient (R^2) of 0.987 were obtained. In order to determine the repeatability and reproducibility, five fabricated thin films were also investigated by extracting water samples spiked with 1 $ngmL^{-1}$ of the digoxin. The RSDs are summarized in Table 1. Based on the data, the method demonstrated good repeatability and reproducibility. The LOD calculated based on the peak-to-peak noise (S/N=3) was 0.003 $ngmL^{-1}$. The lowest concentration of the linear range was considered as the LOQ for each compound (see Table 2). The samples were reused over 50 times while no considerable effect was found on the extraction efficiency (RSD<%2.7). Nevertheless, the samples extraction performance could be altered by releasing the film from the ZnS/MoS_2/cellulose papers within the sample solution in further usage.

Real sample analysis

To assess the method's applicability to determine the examined digoxin in real specimens and investigate the effects of the sample matrix on quantifying, the technique was utilized to analyze plasma and urine samples as a biological specimen. TFME of (a) non-spiked and (b) spiked urine samples with 1 $ngmL^{-1}$ of digoxin were performed,

Table3. The results obtained for the analysis of the spiked water samples (10 ng mL^{-1}) by the proposed method, under the optimized conditions.

Samples	Real(ng mL^{-1})	Added (ng mL^{-1})	Found (ng mL^{-1})	Relative Recovery (%)
Plasma Sample 1	ND	10	10.2	102±2.1
Plasma Sample 2	ND	10	9.7	97±3.6
Urine Sample 1	ND	10	10.1	101±2.8
Urine Sample 2	ND	10	9.6	96±4.3

[a] The relative standard deviations for three replicates.

and HPLC was used for analysis. To evaluate the method's ability in real sample analysis, RSD and relative recovery were regarded in the sample analysis via the technique. Relative recovery was determined as the analyte concentration ratio observed in the real samples compared to that observed in water and spiked at the same concentrations. Relative recoveries acquired for all the specimens were more than 90% (Table 3).

CONCLUSION

In this work, a highly capable, simple, fast, cost-effective, robust, and novel technique was presented to extract and chromatographically determine digoxin in various complex matrices. The cellulose paper was bought from a local supermarket. The in-situ growth of the flower-like ZnS/MoS_2 on the cellulous paper was performed via a simple hydrothermal method. The ZnS/MoS_2 cellulous paper was then used as the TFME sorbent. The method provides some advantages including simplicity, low cost, long sorbent life-time, and short analysis time. In addition, the presented TFME demonstrated a satisfactory reproducibility, low LOD, and wide LDR.

CONFLICT OF INTEREST

The authors declare no conflicts of interest.

REFERENCES

1. Tzou MC, Sams RA, Reuning RH. Specific and sensitive determination of digoxin and metabolites in human serum by high performance liquid chromatography with cyclodextrin solid-phase extraction and precolumn fluorescence derivatization. Journal of Pharmaceutical and Biomedical Analysis. 1995;13(12):1531-40. https://doi.org/10.1016/0731-7085(95)01593-0
2. Chemie GDCFA. Fresenius' Zeitschrift für analytische Chemie: Springer-Verlag; München; 1963.
3. MR P. Digoxin-like immunoreactivity in premature and full-term infants not receiving digoxin therapy. N Engl J Med. 1983;308:904-5. https://doi.org/10.1056/NEJM198304143081516
4. Varma MVS, Kapoor N, Sarkar M, Panchagnula R. Simultaneous determination of digoxin and permeability markers in rat in situ intestinal perfusion samples by RP-HPLC. Journal of Chromatography B. 2004;813(1):347-52. https://doi.org/10.1016/j.jchromb.2004.09.047
5. Jedlička A, Grafnetterová T, Miller V. HPLC method with UV detection for evaluation of digoxin tablet dissolution in acidic medium after solid-phase extraction. Journal of Pharmaceutical and Biomedical Analysis. 2003;33(1):109-15. https://doi.org/10.1016/S0731-7085(03)00226-7
6. Kelly KL, Kimball BA, Johnston JJ. Quantitation of digitoxin, digoxin, and their metabolites by high-performance liquid chromatography using pulsed amperometric detection. Journal of Chromatography A. 1995;711(2):289-95. https://doi.org/10.1016/0021-9673(95)00525-R
7. Gault MH, Longerich L, Dawe M, Vasdev SC. Combined liquid chromatography/ radioimmunoassay with improved specificity for serum digoxin. Clinical Chemistry. 1985;31(8):1272-7. https://doi.org/10.1093/clinchem/31.8.1272
8. González GP, Hernando PF, Durand Alegría JS. Determination of digoxin in serum samples using a flow-through fluorosensor based on a molecularly imprinted polymer. Biosensors and Bioelectronics. 2008;23(11):1754-8. https://doi.org/10.1016/j.bios.2008.01.018
9. González GP, Hernando PF, Alegría JSD. An optical sensor for the determination of digoxin in serum samples based on a molecularly imprinted polymer membrane. Analytica Chimica Acta. 2009;638(2):209-12. https://doi.org/10.1016/j.aca.2009.02.023
10. Øiestad EL, Johansen U, Opdal MS, Bergan S, Christophersen AS. Determination of Digoxin and Digitoxin in Whole Blood. Journal of Analytical Toxicology. 2009;33(7):372-8. https://doi.org/10.1093/jat/33.7.372
11. Abolghasemi MM, Piryaei M. Development of direct microwave desorption/gas chromatography mass spectrometry system for rapid analysis of volatile components in medicinal plants. Journal of Separation Science. 2020;43(4):782-7. https://doi.org/10.1002/jssc.201900821
12. Abolghasemi MM, Piryaei M, Imani RM. Deep eutectic solvents as extraction phase in head-space single-drop microextraction for determination of pesticides in fruit juice and vegetable samples. Microchemical Journal. 2020;158:105041. https://doi.org/10.1016/j.microc.2020.105041
13. Majdafshar M, Piryaei M, Abolghasemi MM, Rafiee E. Polyoxometalate-based ionic liquid coating for solid phase microextraction of triazole pesticides in water samples. Separation Science and Technology. 2019;54(10):1553-9. https://doi.org/10.1080/01496395.2019.1572625

14. Abolghasemi MM, Amirifard H, Piryaei M. Biotemplate route for fabrication of a hybrid material composed of hierarchical boehmite, layered double hydroxides (Mg-Al) and porous carbon on a steel fiber for solid phase microextraction of agrochemicals. Microchimica Acta. 2019;186(10):678. https://doi.org/10.1007/s00604-019-3782-1
15. Abolghasemi MM, Habibiyan R, Jaymand M, Piryaei M. A star-shaped polythiophene dendrimer coating for solid-phase microextraction of triazole agrochemicals. Microchimica Acta. 2018;185(3):179. https://doi.org/10.1007/s00604-017-2639-8
16. Hendi R, Piriyaei M, Babashpour Asl M, Abolghasemi MM. Nanoporous Silica-Polypyrrole/SBA-15 as Fiber Coated in the Solid-Phase Microextraction for Determination of Salvia hydrangea DC. Essential Oil. 2018;24(3):235-9. https://doi.org/10.15171/PS.2018.34
17. Abolghasemi MM, Hassani S, Bamorowat M. Efficient solid-phase microextraction of triazole pesticides from natural water samples using a Nafion-loaded trimethylsilane-modified mesoporous silica coating of type SBA-15. Microchimica Acta. 2016;183(2):889-95. https://doi.org/10.1007/s00604-015-1724-0
18. Abolghasemi MM, Arsalani N, Yousefi V, Arsalani M, Piryaei M. Fabrication of polyaniline-coated halloysite nanotubes by in situ chemical polymerization as a solid-phase microextraction coating for the analysis of volatile organic compounds in aqueous solutions. Journal of Separation Science. 2016;39(5):956-63. https://doi.org/10.1002/jssc.201500839
19. Abolghasemi MM, Parastari S, Yousefi V. Microextraction of phenolic compounds using a fiber coated with a polyaniline-montmorillonite nanocomposite. Microchimica Acta. 2015;182(1):273-80. https://doi.org/10.1007/s00604-014-1323-5
20. Abolghasemi MM, Yousefi V, Piryaei M. Synthesis of a metal-organic framework confined in periodic mesoporous silica with enhanced hydrostability as a novel fiber coating for solid-phase microextraction. Journal of Separation Science. 2015;38(7):1187-93. https://doi.org/10.1002/jssc.201400916
21. Abolghasemi MM, Yousefi V, Piryaei M. Synthesis of carbon nanotube/layered double hydroxide nanocomposite as a novel fiber coating for the headspace solid-phase microextraction of phenols from water samples. Journal of Separation Science. 2015;38(8):1344-50. https://doi.org/10.1002/jssc.201401191
22. Jiang R, Pawliszyn J. Thin-film microextraction offers another geometry for solid-phase microextraction. TrAC Trends in Analytical Chemistry. 2012;39:245-53. https://doi.org/10.1016/j.trac.2012.07.005
23. Bruheim I, Liu X, Pawliszyn J. Thin-Film Microextraction. Analytical Chemistry. 2003;75(4):1002-10. https://doi.org/10.1021/ac026162q
24. Wu H, Qin L, Dong G, Hua M, Yang S, Zhang J. An investigation on the lubrication mechanism of MoS2 nano sheet in point contact: The manner of particle entering the contact area. Tribology International. 2017;107:48-55. https://doi.org/10.1016/j.triboint.2016.11.009
25. Chen M, Dai Y, Wang J, Wang Q, Wang Y, Cheng X, et al. Smart combination of three-dimensional-flower-like MoS2 nanospheres/interconnected carbon nanotubes for application in supercapacitor with enhanced electrochemical performance. Journal of Alloys and Compounds. 2017;696:900-6. https://doi.org/10.1016/j.jallcom.2016.12.077
26. Gomathi PT, Sahatiya P, Badhulika S. Large-Area, Flexible Broadband Photodetector Based on ZnS-MoS2 Hybrid on Paper Substrate. Advanced Functional Materials. 2017;27(31):1701611. https://doi.org/10.1002/adfm.201701611
27. Acerce M, Voiry D, Chhowalla M. Metallic 1T phase MoS2 nanosheets as supercapacitor electrode materials. Nature Nanotechnology. 2015;10(4):313-8. https://doi.org/10.1038/nnano.2015.40